

A Numerical Model for Predicting Diffusivity in a Biocatalyst Particle with Heterogeneous Reactions

Binxin Wu

Philadelphia Mixing Solutions Ltd., Palmyra, PA 17078

Yan Liu and Wei Liao

Dept. of Biosystems and Agricultural Engineering, Michigan State University, East Lansing, MI 48824

Shulin Chen

Dept. of Biological Systems Engineering, Washington State University, Pullman, WA 99164

DOI 10.1002/aic.11542

Published online June 10, 2008 in Wiley InterScience (www.interscience.wiley.com).

Determination of effective diffusivity of a substrate in biocatalyst particles is a key requirement in modeling heterogeneous reactions. The diffusivity is mainly controlled by the molecular-diffusion characteristics of the substrate, the tortuousness of the diffusion path within the biocatalyst, and the void fraction of particle volume available for diffusion. A general numerical model describing reactions in a biocatalyst particle following zero-order, first-order, and Michaelis-Menten kinetics was developed. Finite volume method was used to discretize the nonlinear second-order differential equation, and tridiagonal matrix algorithm was applied to solve the algebraic equation iteratively after discretization. Computer codes were written for calculating the diffusivity under specified boundary conditions. The numerical solution of the diffusion-reaction equations was validated against the experimental data from literatures. The model was further calibrated with experimental data obtained from fungal pellet experiments and then verified using additional data. The results show that the inverse methodology developed in this study was capable of predicting diffusivity in biocatalyst particles. Based on the predicted diffusivity, oxygen consumption by an individual pellet was simulated, oxygen consumptions by small versus large pellets were compared, and the effect of reaction rate on oxygen consumption was evaluated. © 2008 American Institute of Chemical Engineers AIChE J, 54: 2182–2189, 2008

Keywords: biocatalyst particle, mass transfer, numerical simulation, finite volume method, inverse methodology

Introduction

Biocatalyst particles, such as immobilized enzyme particles, bacterial granules, and fungal pellets, have attracted increasing interest in bioprocessing industry due to their high

productivities and possibilities of being reusable.^{1,2} For further enhancing the production performance of a reactor using biocatalyst particles, better understanding the mass transfer of substrate into the particles is critical. It has been reported that diffusion is the predominant mode of mass transfer in biocatalyst particles.³ The rate of diffusion is mainly determined by the diffusivity⁴ (or diffusion coefficient). Although diffusivity is one of the most important parameters for mass transfer of biocatalyst particles, knowledge on this parameter

Correspondence concerning this article should be addressed to S. Chen at chens@wsu.edu.

is limited, because it is relatively difficult to directly determine the mass diffusivity in such biocatalyst particles that have small size and complicated structure. Thus, it is desirable to explore the possibility of using mathematical models as an effective tool for simulating such a diffusion-reaction system and further obtaining the diffusion parameters.³

The conventional methodology for studying diffusion or a diffusion-reaction system is the direct method that gives mass diffusivity and/or rate constants to solve governing equations and further to predict concentration distribution or mass flux in a system.⁵⁻⁷ However, when mass diffusivity is unknown, especially for the biocatalyst particles, which is of the interest of this study, it is impossible to solve for concentrations in the system. Various researchers⁸⁻¹⁵ investigated the mass diffusivity of biological and other engineering materials. These studies involved measuring substrate concentrations to determine the diffusivity. In practice, it is difficult and often costly to measure the concentration distributions within a bioparticle. One alternative approach is to find solutions using an inverse method derived from finite volume method.¹⁶ Judging from the results of several benchmark numerical solutions, the finite volume method appears to offer a number of advantages over equivalent finite element models, because the finite volume solution is conservative and satisfied exactly for each discretization element of the solution domain rather than on an average sense.¹⁷ In addition, the finite volume method has an obvious advantage over a finite difference method if the physical domain is highly irregular and complicated, because arbitrary volumes can be used to subdivide the physical domain.¹⁷ Also, because the integral equations are solved directly in the physical domain, no coordinate transformation is required.¹⁸ Mathematically, the inverse method deals with ill-posed problem in which the solutions do not satisfy the general requirement of existence, uniqueness, and stability under small input changes.^{19,20}

In the study reported herein, an attempt was made to apply an inverse method for estimating the diffusivity of substrate in biocatalyst particles within a heterogeneous reaction system. A random initial value of diffusivity was given first, and then the mass transfer governing equations were solved until the solutions meet the requirements of specified boundary conditions. This study included four parts: (1) development of a general numerical model that describes diffusion-reaction process within a single biocatalyst particle with zero-order, first-order, and Michaelis-Menten reaction kinetics, (2) development of a computer code based upon finite volume method for solving mass diffusivity, (3) verification of finite volume method with experimental data from literature, and (4) validating simulated diffusivities against the results obtained from fungal fermentation experiments.

Model Development

Governing equations

In the development of a diffusion-reaction model, the following assumptions were made:

- A particle is isothermal and spherical;
- Diffusion-reaction process is at steady state;
- The transport of substrate to the particle follows Fick's law;

- The substrate is heterogeneously distributed in the particle;
- The reaction occurs at uniform temperature and pH throughout the biocatalyst particle; and
- The pressure and electrostatic effects are negligible.

Based on the above assumptions, the diffusion-reaction in a spherical biocatalyst particle can be mathematically described as²¹

$$\frac{1}{r^2} \frac{d}{dr} \left(D \frac{dC}{dr} r^2 \right) - \Omega = 0 \quad (1)$$

where C is the concentration of the substrate in the particle (kg/m^3), D is the effective diffusivity of the substrate (m^2/s), r is the distance from the center of the particle (m), and Ω is the reaction rate ($\text{kg/m}^3\text{s}$) that can be expressed as

$$\Omega = \frac{v_{\max} C}{K_m + C} \quad (2)$$

where v_{\max} is the maximum rate of reaction at infinite reactant concentration ($\text{kg/m}^3\text{s}$), and K_m is the Michaelis-Menten constant (kg/m^3). Equation 2 becomes zero-order kinetics at high substrate concentration ($C_s \gg K_m$) and first-order kinetics at low substrate concentration ($C_s \ll K_m$).

Equation 1 is subject to boundary conditions shown in Figure 1a:

$$C|_{r=0} = 0, \quad \text{or} \quad \frac{dC}{dr} \Big|_{r=0} = 0 \quad (3)$$

and

$$C|_{r=R} = C_s, \quad \text{or} \quad \frac{dC}{dr} \Big|_{r=R} = \frac{k_1}{D} (C_1 - C_i) \quad (4)$$

where k_1 is external mass transfer coefficient (m/s), C_1 is the substrate concentration in bulk liquid (kg/m^3), and C_i is the substrate concentration at the particle surface (kg/m^3).

Finite volume method

For solving the governing equations, Eq. 1 can be written in a general form as

$$\frac{d}{dr} \left(D \frac{dC}{dr} r^2 \right) + S(r) = 0 \quad (5)$$

where

$$S(r) = -\frac{v_{\max} C}{K_m + C} r^2 \quad (6)$$

Equation 5 is a nonlinear second-order differential equation that cannot be analytically solved. Thus, the finite volume method will be used to transform Eq. 5 into algebraic form that can be iteratively solved.¹⁶

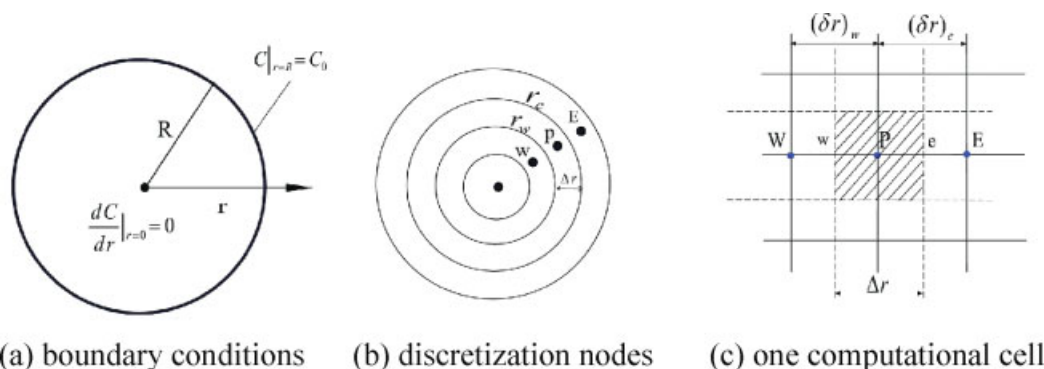


Figure 1. Schematic of control volume for a pellet in the spherical coordinate system.

[Color figure can be viewed in the online issue, which is available at www.interscience.wiley.com.]

Integrating the first term in Eq. 5 along the control volume (Figures 1b, c) yields

$$\int_w^e \frac{d}{dr} \left(D \frac{dC}{dr} r^2 \right) dr = \frac{Dr_e^2}{\delta r_e} C_E + \frac{Dr_w^2}{\delta r_w} C_W - \left(\frac{Dr_e^2}{\delta r_e} + \frac{Dr_w^2}{\delta r_w} \right) C_P \quad (7)$$

Integrating the second term in Eq. 5 along the control volume (Figures 1b, c) yields

$$\int_w^e -\frac{v_{\max} C}{K_m + C} r^2 dr = -\frac{1}{3} (r_e^3 - r_w^3) \frac{v_{\max} C_P}{K_m + C_P} \quad (8)$$

The algebraic equation after discretization can be expressed as

$$a_P C_P = a_E C_E + a_W C_W + b \quad (9)$$

where

$$a_E = Dr_e^2 / \delta r_e, \quad a_W = Dr_w^2 / \delta r_w, \quad a_P = a_E + a_W; \quad b = -\frac{1}{3} (r_e^3 - r_w^3) \frac{v_{\max} C_P}{K_m + C_P} \quad (10)$$

Equation 9 can be solved using tridiagonal matrix algorithm. The solution procedure includes (1) giving the initial concentration distributions, (2) solving Eq. 9 to obtain the updated concentrations, and (3) substituting the updated values for the initial ones in Eq. 9 and repeating the calculations until convergence the criterion are satisfied.

Solution procedure for predicting diffusivity

The solution procedure for predicting diffusivity includes the following steps:

1. Setting $\varepsilon = 0$;
2. Inputting the particle radius, and specifying boundary conditions in which $C|_{r=0} = 0$, and $C|_{r=R} = C_s$;
3. Giving an initial value of diffusivity (e.g., $D^0 = 1 \times 10^{-8} \text{ m}^2/\text{s}$) and setting a decrement value of diffusivity (e.g., $\Delta D = 1 \times 10^{-11} \text{ m}^2/\text{s}$);
4. Solving Eq. 1 using finite volume method to obtain the concentration distributions inside the particle;
5. If the concentration at central point is greater than zero ($C|_{r=0} > \varepsilon$), then update diffusivity by calculating $D = D^0 - \Delta D$, and go back to step 4 until $C|_{r=0} \leq \varepsilon$.

Verification of finite volume method

Finite volume method is the core of the solution procedure developed in this study for predicting diffusivity. Thus, this method has to be verified prior to further application for predicting diffusivity of various biocatalyst particles. For zero- and first-order kinetics, Eq. 1 has analytical solutions under Neumann and Dirichlet boundary conditions.³ For Michaelis-Menten kinetics, however, Eq. 1 can only be numerically solved. To verify the numerical solutions, the experimental data from Hooijman et al.²² were used. This literature²² used an oxygen microsensor to measure internal oxygen profiles in biocatalyst particles of different diameter and activity. The parameters from the model system of oxygen consuming enzyme immobilized in a carrier material were as follows:

- Two enzyme concentration = 0.0025 and 0.005 kg/m³;
- Particle diameter = 5.0 mm;
- Substrate concentration = 0.2 mol/m³;
- Effective mass diffusivity = $2.3 \times 10^{-9} \text{ m}^2/\text{s}$;
- External mass transfer coefficient = $4.4 \times 10^{-5} \text{ m/s}$;
- $K_m = 0.005 \text{ mol/m}^3$ for $E = 0.0025 \text{ kg/m}^3$, $K_m = 0.011 \text{ mol/m}^3$ for $E = 0.005 \text{ kg/m}^3$;

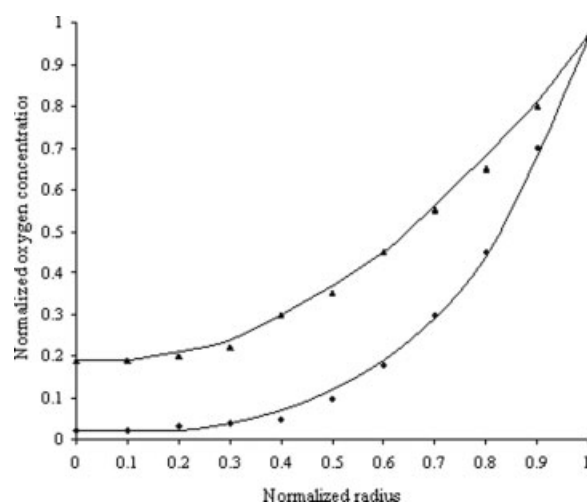
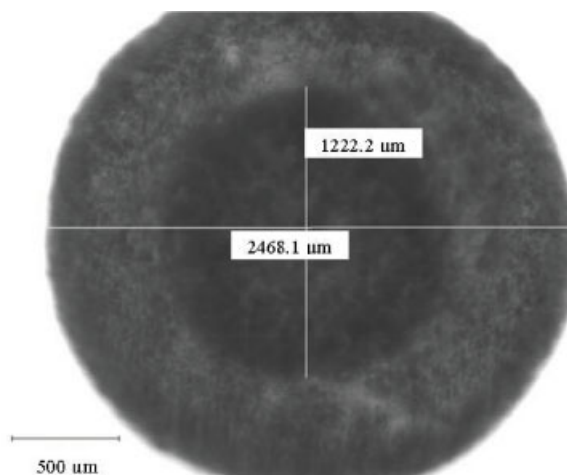


Figure 2. Influence of enzyme concentration (E) on oxygen profiles following the measured data²²: $E = 0.0025 \text{ kg/m}^3$ (\blacktriangle), $E = 0.005 \text{ kg/m}^3$ (\blacklozenge), and the fitted prediction curves (—).



(a) *R. Oryzae* pellet



(b) Light microscopy of a *R. Oryzae* pellet

Figure 3. Experiments of fungal pellets.

[Color figure can be viewed in the online issue, which is available at www.interscience.wiley.com.]

- $v_{\max} = 0.15 \text{ mol/kg}$ for $E = 0.0025 \text{ kg/m}^3$, $v_{\max} = 0.113 \text{ mol/kg}$ for $E = 0.005 \text{ kg/m}^3$.

In this literature, $\Omega = \frac{E v_{\max} C}{K_m + C}$, and Neumann and Robin boundary conditions were applied to the particle center ($\frac{dC}{dr}|_{r=0} = 0$) and particle surface ($\frac{dC}{dr}|_{r=R} = \frac{k_1}{D}(C_1 - C_i)$), respectively.

Model application—prediction of oxygen consumption for an individual pellet

According to Fick's law, the mass flux of oxygen inside a pellet, J , can be calculated as

$$J = D \frac{dC}{dr} A(r) \quad (11)$$

where $A(r)$ is the spherical surface area at radius r , which can be expressed as

$$A(r) = 4\pi r^2 \quad (12)$$

$A(r)$ is calculated as a spherical surface area with the mean radius between two successive nodes. Equations 11 and 12 allow the calculation of total oxygen consumption by an individual pellet.

Fungal Pellet Fermentation Experiments

Two pelletized fungal fermentation experiments were independently conducted for calibrating the model and validating the result. Fungus *Rhizopus oryzae* NRRL 395 (ATCC

9363), obtained from the American Type Culture Collection (Manassas, VA), was used in the study. The fungal pellets were formed using the method described in Liu et al.¹ A completely randomized design with four replicates of six cultures was used to study the effects of the seed sizes and inoculums on oxygen transfer during cultivation. Two pellet sizes (0.73 ± 0.11 and 1.04 ± 0.17) and three inoculums (2, 4, and 10%) were studied. For each individual treatment, 50 mL of potato dextrose broth with additional glucose concentration 100 g/L was added into a 125-mL flask. Calcium carbonate was used to keep the pH at 5. The cultures were processed for 2 days at 27°C using an orbital shaker (Classic Series C24 Incubator shaker, New Brunswick Scientific, Edison, NJ) at 170 rpm. The dissolved oxygen (DO) concentration of each flask was measured immediately using a DO meter after the flask was taken off from the shaker.

To verify the results of diffusivity prediction in a fungal pellet, measurements of substrate concentration, reaction rate, and diameters of pellet and cavity (where DO is zero) inside the pellet were conducted (Figure 3).

Results and Discussion

Verification with immobilized oxygen reducing enzyme experiments

The numerical simulations obtained based on finite volume method were verified with the experimental data of Hooij-

Table 1. Experimental Runs and Results Used to Predict Diffusivity

Run	Seed Size [$\times 10^3$ (m)]	Inoculums (%)	$R \times 10^3$ (m)	$r \times 10^3$ (m)	$C_s \times 10^3$ (kg/m ³)	$k_0 \times 10^3$ (kg/m ³ s)	Predicted $D \times 10^{10}$ (m ² /s)
1	0.73 ± 0.11	2	1.65	0.6	6.4	0.0085	2.4
2	0.73 ± 0.11	4	1.08	0.38	6.56	0.041	5.0
3	0.73 ± 0.11	10	0.69	0	6.55	0.035	4.1
4	1.04 ± 0.17	2	1.32	0.36	6.4	0.014	3.3
5	1.04 ± 0.17	4	1.09	0.42	6.39	0.012	1.3
6	1.04 ± 0.17	10	1.21	0.66	5.75	0.015	1.2

Table 2. Diffusivity and Oxygen Concentrations in a Fungal Pellet at Each Computational Node with Respect to Iterations

<i>I</i>	$D \times 10^{10} \text{ (m}^2/\text{s)}$	Oxygen Concentration [$\times 10^3 \text{ (kg/m}^3)$]										
		C(1)	C(2)	C(3)	C(4)	C(5)	C(6)	C(7)	C(8)	C(9)	C(10)	C(11)
1	100.0	6.2	6.2	6.3	6.3	6.3	6.3	6.3	6.3	6.3	6.4	6.4
100	90.1	6.2	6.2	6.2	6.2	6.3	6.3	6.3	6.3	6.3	6.4	6.4
200	80.1	6.2	6.2	6.2	6.2	6.2	6.3	6.3	6.3	6.3	6.4	6.4
300	70.1	6.2	6.2	6.2	6.2	6.2	6.2	6.3	6.3	6.3	6.4	6.4
400	60.1	6.1	6.1	6.2	6.2	6.2	6.2	6.2	6.3	6.3	6.4	6.4
500	50.1	6.1	6.1	6.1	6.1	6.1	6.2	6.2	6.2	6.3	6.3	6.4
600	40.1	6.0	6.0	6.0	6.0	6.1	6.1	6.2	6.2	6.3	6.3	6.4
700	30.1	5.9	5.9	5.9	5.9	6.0	6.0	6.1	6.1	6.2	6.3	6.4
800	20.1	5.6	5.6	5.7	5.7	5.7	5.8	5.9	6.0	6.1	6.3	6.4
900	10.1	4.9	4.9	4.9	5.0	5.1	5.2	5.4	5.6	5.8	6.1	6.4
950	5.1	3.4	3.4	3.5	3.6	3.8	4.1	4.4	4.8	5.3	5.8	6.4
960	4.1	2.6	2.6	2.7	2.9	3.2	3.5	4.0	4.5	5.0	5.7	6.4
970	3.1	1.4	1.4	1.6	1.8	2.2	2.6	3.2	3.8	4.6	5.4	6.4
971	3.0	1.3	1.3	1.4	1.7	2.0	2.5	3.1	3.7	4.5	5.4	6.4
972	2.9	1.1	1.1	1.2	1.5	1.9	2.4	3.0	3.7	4.5	5.4	6.4
973	2.8	0.9	0.9	1.1	1.3	1.7	2.2	2.8	3.6	4.4	5.3	6.4
974	2.7	0.7	0.7	0.9	1.1	1.5	2.1	2.7	3.5	4.3	5.3	6.4
975	2.6	0.5	0.5	0.6	0.9	1.4	1.9	2.6	3.3	4.2	5.3	6.4
976	2.5	0.2	0.2	0.4	0.7	1.2	1.7	2.4	3.2	4.2	5.2	6.4
977	2.4	0.0	0.1	0.2	0.5	0.9	1.5	2.2	3.1	4.1	5.2	6.4

Note: Setting the initial test value of D as $1.0 \times 10^{-8} \text{ m}^2/\text{s}$ and the decrement as $1.0 \times 10^{-11} \text{ m}^2/\text{s}$. The solution of D converges at 977 iterations, and its value is $2.4 \times 10^{-10} \text{ m}^2/\text{s}$.

man et al.²² Figure 2 represents the normalized oxygen concentration versus normalized radius for two different enzyme concentrations. It is clear that the prediction curves fit the measured data favorably. This demonstrates that finite volume method is capable of simulating diffusion-reaction system of various biocatalyst particles with high precision ($r^2 = 0.97$).

Prediction of diffusivity in fungal pellets

The predicted diffusivities by using the model for the six experimental runs were given in the last column of Table 1. These data, ranging from 1.2×10^{-10} to $5.0 \times 10^{-10} \text{ m}^2/\text{s}$, demonstrate that the diffusivities are significantly influenced by the cultivation conditions such as seed pellet size and inoculum. With the seed pellet size of 1.04 mm, the predicted diffusivities for 2, 4, and 10% of inoculum were 3.3×10^{-10} , 1.3×10^{-10} , and $1.2 \times 10^{-10} \text{ m}^2/\text{s}$, respectively. However, with the seed pellet size of 0.73 mm, predicted diffusivities for 2, 4, and 10% of inoculum were 2.4×10^{-10} , 5.0×10^{-10} , and $4.1 \times 10^{-10} \text{ m}^2/\text{s}$, respectively. The diffusivity generally decreases with the increase in inoculum size.

Each of the diffusivity prediction presented in Table 1 was a result of many iterative calculations. An example of the iterative procedure for calculating the diffusivity is shown in Table 2 (as for Run 1 in Table 1). The iterations continue

until, at all computational nodes, the absolute change in oxygen concentration between two successive iterations becomes less than the specified tolerance (10^{-3} in this case). The data in Table 2 indicate that the diffusivity of $2.4 \times 10^{-10} \text{ m}^2/\text{s}$ is converged when the iteration reaches at $I = 977$. It also needs to point out that during the study, it was assumed that (1) a fungal pellet is a spherical particle, (2) oxygen from particle surface diffuses to the interior without external mass transfer, and (3) the cavity inside the pellet is solely caused by lack of oxygen.

Experimental validation of diffusivity on fungal pellet and oxygen consumption estimation

The validation of the prediction was made by comparing the predicted radius of the cavity (r) with measured r in each fungal pellet. When the DO concentration became zero, no oxygen was available to support fungal function. The fungus would die and cavity was created in the pellet. Table 3 shows the results of six sets of comparisons between the predicted and measured r for each D obtained from Table 1. The relative errors between experimental results and predicted r range from 0 to 37.3%. Taken Run 1 as an example, the change in oxygen concentrations in this pellet with the radius are shown in Table 4. The simulated $r = 4.2 \times 10^{-4} \text{ m}$ is close to the measured $r = 4.5 \times 10^{-4} \text{ m}$. For Run 3, it

Table 3. Experiments Used to Validate Diffusivity (D) by Comparison of Measured and Predicted Radius (r)

Run	Seed size [$\times 10^3 \text{ (m)}$]	Inoculums (%)	$R \times 10^3$ (m)	$r \times 10^3$ (m)	$C_s \times 10^3$ (kg/m ³)	$k_0 \times 10^3$ (kg/m ³ s)	$D \times 10^{10}$ (m ² /s)	Predicted $r \times 10^3 \text{ (m)}$	Error (%)
1	0.73 ± 0.11	2	1.44	0.45	6.4	0.009	2.4	0.42	6.7
2	0.73 ± 0.11	4	1.12	0.38	6.87	0.0302	5.0	0.29	23.6
3	0.73 ± 0.11	10	0.7	0	6.75	0.0102	4.1	0	0
4	1.04 ± 0.17	2	1.55	n/a	6.95	n/a	3.3	n/a	n/a
5	1.04 ± 0.17	4	1.21	0.51	7.04	0.0212	1.3	0.70	37.3
6	1.04 ± 0.17	10	1.11	0.55	6.64	0.0256	1.2	0.68	23.6

Table 4. Model Predictions and Experimental Validation as an Example of a Pellet

$C \times 10^3$ (kg/m ³)	$r \times 10^3$ (m), Prediction	$r \times 10^3$ (m), Experiment
0	0.0	0.0
0	0.42	0.45
0.1	0.52	N/A
0.2	0.63	N/A
0.5	0.73	N/A
0.9	0.83	N/A
1.5	0.93	N/A
2.2	1.03	N/A
3.1	1.13	N/A
4.1	1.24	N/A
5.2	1.34	N/A
6.4	1.44	1.44

Note: The concentrations within $0.45 \text{ mm} < r < 1.44 \text{ mm}$ was not shown due to the fact that only the radius of cavity inside the pellet was used to validate the predictions.

was observed that $r = 0$, indicating that there should be no cavity in this pellet. This observation matches the predicted results from Run 3 in Table 1 perfectly. These results elucidate that the model is valid to predict the diffusivity of fungal pellet. Once the diffusivity of a biocatalyst particle is obtained and the model is validated, the model may have many practical applications. One example is the estimation of oxygen consumption by a pellet according to Eqs. 11 and 12. In Run 1, for instance, $\bar{r} = 0.47 \text{ mm}$ represents a spherical surface between the node with $r = 0.42 \text{ mm}$ and the node with $r = 0.52 \text{ mm}$ as shown in Table 4, respectively. The concentration gradient and mass flux of oxygen between two successive nodes are presented in Table 5. The total oxygen consumption in the pellet for Run 1 was estimated as $2.842 \times 10^{-13} \text{ kg/s}$.

Comparisons of oxygen consumptions for fungal pellets with different sizes

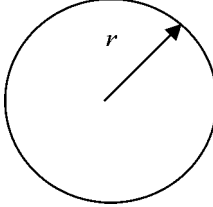
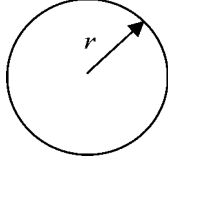
Desirable pellet size is an important topic in fungal fermentation. In principle, the smaller the particle is, the more desirable it will be. Nonetheless, quantifying performance differences between large and small pellets provide very important information. Table 6 shows the oxygen consumptions for a larger pellet versus a smaller one. In obtaining these

Table 5. Predictions of Oxygen Consumption in a Pellet

$r \times 10^3$ (m)	$dC \times 10^3$ (kg/m ³)	$J \times 10^{14}$ (kg/s)
0.21	0.0	0.0
0.47	0.1	0.098
0.57	0.1	0.135
0.67	0.3	0.536
0.77	0.4	0.913
0.87	0.6	1.702
0.97	0.7	2.416
1.07	0.9	3.714
1.17	1.0	4.862
1.27	1.1	6.223
1.37	1.2	7.817

Note: Total oxygen consumption = $2.842 \times 10^{-13} \text{ kg/s}$.

Table 6. Comparisons of Oxygen Consumptions in Small and Large Pellets

Large Pellet	Small Pellet
$V = 25 \times 10^{-6} \text{ m}^3$, $r = 1.81 \times 10^{-3} \text{ m}$	$V = 12.5 \times 10^{-6} \text{ m}^3$, $r = 1.44 \times 10^{-3} \text{ m}$
	
Oxygen consumption $\times 10^{13}$ (kg/s) 4.807	2.842

results, it was assumed that one large pellet has the equivalent volume of two small pellets, and both pellets have the same density. Given the small pellet radius of 1.44 mm from Run 1 in Table 3, the radius of a large pellet was calculated as 1.81 mm . From Eqs. 11 and 12, it can be found that the mass flux (J) is directly proportional to diffusivity (D), concentration gradient (dC/dr), and the spherical surface area through which the oxygen diffuses ($A(r)$). As diffusion occurs from the outer layer to the inner layers of each pellet, the more the surface area, the more the mass flux. Because the surface area of two small pellets are greater than that of the large one based on the same pellet volume, the ratio of oxygen consumption of two small ones to that of the large one is about 1.18, which indicates that the small pellets have higher substrate consumption, thus high reaction rate.

For zero-order kinetics of spherical particle, the maximum particle radius without cavity, R_{\max} , can be calculated using Eq. 13³:

$$R_{\max} = \sqrt{\frac{6DC_s}{k_0}} \quad (13)$$

The relationships between R_{\max} and k_0 are presented in Figure 4. The pellet size decreases following the increase of reaction rate, whereas it increases following the increase of diffusivity. The data also show that the oxygen consumption rate needs to be maintained at $3.6 \times 10^{-6} \text{ kg/m}^3 \text{ s}$ for avoiding the oxygen limitation for the pellets less than 1.6 mm (Figure 4). As presented in the previous section, the oxygen consumption rate k_0 from Run 1 in Table 3 is $9.0 \times 10^{-6} \text{ kg/m}^3 \text{ s}$ higher than $3.6 \times 10^{-6} \text{ kg/m}^3 \text{ s}$, which means that oxygen consumption was faster than oxygen diffusion into the pellets. Cavity was then observed inside the pellets with a radius of 0.45 mm . On the other hand, small pellets of 0.7 mm at the diffusivity of $4.1 \times 10^{-10} \text{ m}^2/\text{s}$ had the k_0 of $10.2 \times 10^{-6} \text{ kg/m}^3 \text{ s}$ (Run 3 in Table 3) that was much less than the required k_0 of $30 \times 10^{-6} \text{ kg/m}^3 \text{ s}$ (Figure 4, D3). This result suggests that there would be no oxygen limitation for the small pellets of 0.7 mm , which is further proved by the observation of lacking cavity inside of the pellets (Table 3).

Oxygen transfer is always one of the major limitations associated with aerobic fermentation with pelletized fungus. Although certain level of oxygen is needed to maintain the

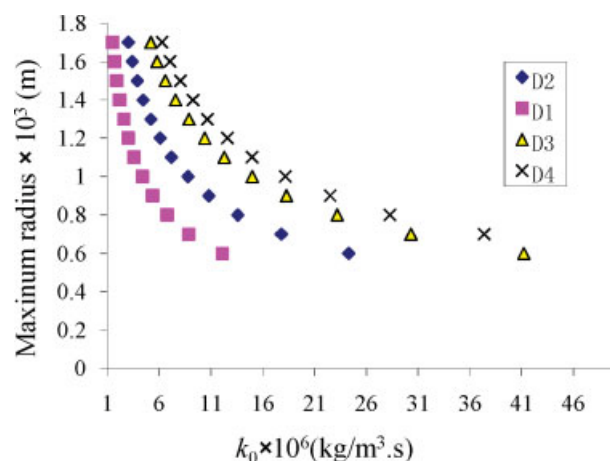


Figure 4. Oxygen consumption rate versus different pellet size*.

*D1 = 1.2×10^{10} (m²/s); D2 = 2.4×10^{10} (m²/s); D3 = 4.1×10^{10} (m²/s); D4 = 5.0×10^{10} (m²/s), and bulk oxygen concentration at 6×10^{-6} kg/m³. [Color figure can be viewed in the online issue, which is available at www.interscience.wiley.com.]

activity of fungal biomass to produce the target products, excessive aeration and agitation require high equipment cost and input of energy thus needs to be minimized. Controlling oxygen to the optimal level is often a great challenge for the design and operations of aerobic fungal fermentation. The model developed in this study provides an effective tool for simulating oxygen transfer in fungal pellets. The oxygen transfer modeling, along with kinetic analysis of pelletized fungal fermentation, could eventually lead to the development of optimal fungal fermentation processes with the maximal production rate and least energy consumptions.

The above results and discussions also suggest that the proposed methodology in this study could serve as an example for the future research on dealing with inverse problems in the bioengineering field.

Conclusions

The following conclusions can be drawn from this study:

1. A general inverse methodology based on finite volume method was capable of predicting diffusivity in a biocatalyst particle with heterogeneous reactions;
2. Numerical solutions of the above model using finite volume method agreed with both experimental results and results from literatures;
3. Predictions using the model quantitatively verified that smaller pellet size was superior to large ones in aerobic fungal fermentation process in terms of mass transfer rate.

Acknowledgments

The authors thank the IMPACT program of Washington State University and the Paul G. Allen Foundation for providing the financial support for this research.

Notation

A = spherical surface area, m²
a = coefficient in the algebraic equation

b = coefficient in the algebraic equation
C = concentration, kg/m³ or mol/m³
D = diffusivity, m²/s
E = enzyme
I = iterations
J = mass flux, kg/s
k₀ = zero-order kinetics, kg/m³ s
k₁ = external mass transfer coefficient, m/s
K_m = Michaelis-Menten constant, kg/m³
R = radius, m
r = radius, m
S = source term
V = volume, m³

Greek letters

Ω = reaction rate, kg/m³ s
v_{max} = maximum rate of reaction, kg/m³ s
ε = reference value

Superscript

0 = initial value

Subscripts

e, w = east and west faces of the control volume
E, W = east and west nodes relative to central node, P
i = particle surface
l = bulk liquid
P = central node of the control volume.
s = substrate.

Literature Cited

1. Liu Y, Liao W, Liu C, Chen S. Optimization of L-(+)-lactic acid production using palletized filamentous *Rhizopus oryzae* NRRL 395. *Appl. Biochem. Biotechnol.* 2006;129–132:844–853.
2. Van Sijidam JC, Kossen NWF, Paul PG. An inoculum technique for the production of fungal pellets. *Eur. J. Appl. Microbiol. Biotechnol.* 1980;10:211–221.
3. Doran PM. *Bioprocess Engineering Principles*. New York: Academic Press, 1995.
4. Stewart PS. A review of experimental measurements of effective diffusivity permeabilities and effective diffusion coefficients in biofilms. *Biotechnol. Bioeng.* 1998;59:261–272.
5. Cui YQ, Okkerse WJ, van der Lans RGJM, Luyben KChAM. Modeling and measurements of fungal growth and morphology in submerged fermentations. *Biotechnol. Bioeng.* 1998;60:216–229.
6. Gutenwik J, Nilsson B, Axelsson A. Mass transfer effects on the reaction rate for heterogeneously distributed immobilized yeast cells. *Biotechnol. Bioeng.* 2002;79:664–673.
7. Chowdhury BR, Chakraborty R, Chaudhuri UR. Modeling and simulation of diffusional mass transfer of glucose during fermentative production of pediocin AcH from *Pediococcus acidilactici* H. *Biomed. Eng. J.* 2003;16:237–243.
8. Beer DD, Heuvel JCVD. Gradients in immobilized biological systems. *Anal. Chim. Acta* 1988;213:259–265.
9. Chresand TJ, Dale BE, Hanson SL. A stirred bath technique for diffusivity measurements in cell matrices. *Biotechnol. Bioeng.* 1988;32:1029–1036.
10. Pu HT, Yang RYK. Diffusion of sucrose and yohimbine in calcium alginate gel beads with or without entrapped plant cells. *Biotechnol. Bioeng.* 1988;32:891–896.
11. Scott CD, Woodward CA, Thompson JE. Solute diffusion in biocatalyst gel beads containing biocatalyst and other additives. *Enzyme Microb. Technol.* 1989;11:258–263.
12. Davies AJ, Christianson DB, Dixon LC, Roy R, van der Zee P. Reverse differentiation and inverse diffusion problem. *Adv. Eng. Softw.* 1997;28:217–221.
13. Ji X, Kritiphat W, Aboudheir A, Tontiwachwuthikul P. Mass transfer parameter estimation using optimization technique: case study in CO₂ absorption with chemical reaction. *Can. J. Chem. Eng.* 1999;77:69–73.

14. Liu JY, Simpson WT, Verrill SP. An inverse moisture diffusion algorithm for the determination of diffusion coefficient. *Dry. Technol.* 2001;19:1555–1568.
15. Vasconcellos JFV, Neto AJS, Santana CC. An inverse mass transfer problem in solid-liquid adsorption system. *Inverse Probl. Eng.* 2003;11:391–408.
16. Patankar SV. *Numerical Heat Transfer and Fluid Dynamics*. New York: Hemisphere, 1980.
17. Bijelonja I, Demirdžić I, Muzaferija S. A finite volume method for incompressible linear elasticity. *Comput. Methods Appl. Mech. Eng.* 2006;195:6378–6390.
18. Tannehill J, Anderson D, Pletcher R. *Computational Fluid Mechanics and Heat Transfer*, 2nd ed. New York: Hemisphere, 1997.
19. Beck JV, Blackwell B, Clair CRST Jr. *Inverse Heat Conduction*. New York: Wiley, 1985.
20. Ozisik MN. *Heat Conduction*. New York: Wiley, 1993.
21. Crank J. *The Mathematics of Diffusion*, 2nd ed. London: Oxford University Press, 1975.
22. Hooijman CM, Geraats SGM, Luyben KCAM. Use of an oxygen microsensor for the determination of intrinsic kinetic parameters of an immobilized oxygen reducing enzyme. *Biotechnol. Bioeng.* 1990;35:1078–1087.

Manuscript received Aug. 28, 2007, revision received Feb. 20, 2008, and final revision received May 3, 2008.